Sensor and Simulation Note

Note 171

March 1973



# Capacitance Bounds for Geometries Corresponding to an Advanced Simulator Design

M. I. Sancer and A. D. Varvatsis
Northrop Corporate Laboratories
Pasadena, California

## Abstract

The capacitance bounds obtained in this note are the capacitance values between surfaces that can be inscribed within or circumscribed about the actual surfaces corresponding to an advanced simulator design. This method of obtaining bounds allows one to compare the capacitance of certain geometries without even making a numerical calculation; however, numerical calculations can readily be performed for arbitrary geometries. To augment our method of obtaining bounds, we determine the capacitance between two noncencentric spheres. This capacitance is in the form of an infinite series and it is numerically summed and plotted. A closed form approximation to this series is also obtained and its accuracy is demonstrated by plotting it for the same range of parameters that were used for the plots of the numerical sum.

# I. Introduction

In this note we present a method for obtaining upper and lower bounds on the capacitance between two perfectly conducting closed surfaces with one of the surfaces enclosing the other (see figure 1). The reason for considering this geometry is that the inner surface represents a space system and the outer surface represents a test chamber in an advanced simulator design. This type of simulator as well as the significance of the capacitance is discussed in a note by Baum [1].

The bounds that we obtain are interpreted as the capacitance between surfaces that can be either inscribed within or circumscribed about the original surfaces. These surfaces are quite general and can be chosen so that the capacitance between them is either known or can be readily calculated. The fact that these bounds can be obtained without specific regard to sharp edges that might exist on the actual surfaces supports the effective radius approximation proposed by Baum [1]. Our results are also consistent with the recent study of Latham [2] concerning the effective radius approximation. He obtains a criterion for the validity of this approximation that primarily depends on the relative size of the two actual surfaces.

Our method of obtaining capacitance bounds is not necessarily the most precise; however, this possible limitation is compensated for by the ease with which bounds can be determined as well as the physical insight that one can obtain without even making a numerical calculation. There is an extensive literature on obtaining capacitance bounds. Two often quoted references which contain methods for obtaining precise capacitance bounds are the book by Pólya and Szegö [3] and the paper by Parr [4].

We calculate the capacitance between one class of surfaces that can always be inscribed within or circumscribed about the surfaces depicted in figure 1. This is the class of nonconcentric spheres. The capacitance between nonconcentric spheres is well known [5] and it appears in the form of an infinite series. In this note we numerically sum this series and analytically approximate this sum. Our analytic approximation results from summing an upper bound for each term in the original series and a simple closed form algebraic expression is obtained. This approximation to the actual capacitance is necessarily an upper bound; however, it also turns out to be an excellent approximation. This is shown in plots of the numerical summation and the approximate expression.

## II. Determination of Capacitance Bounds

Consider the three surfaces depicted in figure 2 and denote the capacitance between $S_i$ and $S_j$ as $C_{ij}$. First we would like to prove the following inequalities

$$C_{13} \le C_{12} \tag{1}$$

and

$$C_{13} \le C_{23} \tag{2}$$

In order to prove these inequalities we use the following two relationships which will be proved in the appendix. The first is

$$C_{ij} = \varepsilon \int_{R_{ij}} |\nabla\phi|^2 d\underline{r} \tag{3}$$

where $\varepsilon$ is the homogeneous dielectric permittivity of the region between the original surfaces in figure 1. $R_{ij}$ is the volume between $S_i$ and $S_j$ and $\phi$ satisfies the conditions

$$\nabla^2\phi(\underline{r}) = 0 \qquad \underline{r} \in R_{ij} \tag{4}$$

and

$$\phi(\underline{r}) = 1 \qquad \underline{r} \in S_i \tag{5a}$$

$$\phi(\underline{r}) = 0 \qquad \underline{r} \in S_j \tag{5b}$$

The other relationship is the inequality

$$C_{ij} \le \varepsilon \int_{R_{ij}} |\nabla\psi|^2 d\underline{r} \tag{6}$$

where

$$\psi(\underline{r}) = 1 \qquad \underline{r} \in S_i \tag{7a}$$

$$\psi(\underline{r}) = 0 \qquad \underline{r} \in S_j \tag{7b}$$

but $\psi$ does not have to satisfy Laplace's equation in $R_{ij}$. Let us now choose a function $\psi$ so that $\psi = 1$ on $S_1$ and $\psi = 0$ on $S_3$. We further require that $\nabla^2\psi(\underline{r}) = 0$ for $\underline{r}\varepsilon R_{12}$ and that $\psi(\underline{r}) = 0$ for $\underline{r}\varepsilon R_{23}$. The preceeding requirements cause $\nabla\psi$ to be discontinuous at $S_2$ so that $\nabla^2\psi \equiv \nabla\cdot(\nabla\psi)$ behaves like a delta function at this boundary. It should be noted that $\psi$ conforms to the appropriate class of functions discussed in the appendix since among the other requirements its first derivatives are piecewise continuous in $R_{13}$. Physically this delta function is the surface charge density induced on $S_2$ so that in $R_{13}$, $\psi$ satisfies a Poisson's equation rather than Laplace's equation, the source term being the induced surface charge density on $S_2$. Using (6) and (7) we have

$$C_{13} \leq \varepsilon \int_{R_{13}} |\nabla\psi|^2 d\underline{r} \tag{8}$$

and because of the definition of $\psi$ and (3) thru (5)

$$\varepsilon \int_{R_{13}} |\nabla\psi|^2 d\underline{r} = \varepsilon \int_{R_{12}} |\nabla\psi|^2 d\underline{r} = C_{12} \tag{9}$$

Combining (8) and (9) we prove the relation given in (1). The relation given in (2) is proved in exactly the same manner. We choose $\psi$ so that $\nabla^2\psi = 0$ in $R_{23}$, $\psi = 0$ in $R_{12}$, $\psi = 1$ on $S_3$, and $\psi = 0$ on $S_2$. We omit the details and assume that (2) has now been proved.

We will now interpret (1) and (2) so as to obtain a procedure to calculate bounds when one of the physical surfaces depicted in figure 1 has a simple geometric shape that is amenable to a capacitance calculation of the type now to be described. Let us assume, for now, that the outer surface in figure 1 has a simple geometric shape, for example consider it to be a sphere. Consider that the inner surface is irregular and imagine a sphere inscribed within it as well as a sphere circumscribed about it. The capacitance between two spheres, not necessarily concentric, is known and will be treated numerically in this note.

Considering $S_2$ to be the actual inner surface and $S_1$ the inscribed shpere, it follows from (1) that the readily calculated capacitance $C_{13}$ is a lower bound on the actual capacitance $C_{12}$. Now consider $S_1$ to be the actual inner surface and $S_2$ to be the circumscribed sphere. From (2) we see that the readily calculated capacitance $C_{23}$ is an upper bound on the actual capacitance $C_{13}$.

We have shown how bounds on the capacitance between $S_3$ and an interior surface can be found by calculating the capacitance between $S_3$ and two other geometrically simple interior surfaces. The upper bound is the capacitance between $S_3$ and the surface that circumscribed the inner surface and the lower bound is the capacitance between $S_3$ and the surface inscribed within the actual inner surface. There is no requirement that either the inscribed or circumscribed surface be spheres. The only requirement for this procedure to be useful is that the bounding capacitances be either known or readily calculated. There is also no requirement that $S_3$ be finite. By considering $S_3$ to become infinite (1) and (2) can be used to provide bounds on the capacitance to infinity of a single surface. The lower bound is the capacitance to infinity of an inscribed surface and the upper bound is the capacitance to infinity of a circumscribed surface. When it is convenient to consider ellipsoidal shapes as the inscribing and circumscribing surfaces, a note by Shumpert [6] should prove useful since it contains numerical values for the capacitance to infinity for this class of surfaces.

It should be noted that (1) and (2) are also directly useful when the inner surface depicted in figure 1 has a simple geometric shape. For this case we consider convenient surfaces inscribed within and circumscribed about the outer surface. An upper bound on the actual capacitance is the capacitance between the actual inner surface and the inscribed surface while a lower bound is the capacitance between the actual inner surface and the circumscribing surface.

We now consider the case where neither of the surfaces in figure 1 have a simple or convenient geometric shape. The analysis of this is facilitated by considering the four surfaces depicted in figure 3. We consider only three surfaces at a time and use (1) and (2) to obtain our bounds. Eliminating $S_2$ we obtain

$$C_{14} \leq C_{13} \tag{10}$$

Eliminating $S_4$ we obtain

$$C_{13} \leq C_{23} \tag{11}$$

Combining (10) and (11) we obtain our desired result. It is

$$C_{14} \leq C_{23} \tag{12}$$

This relationship is used to provide both upper and lower bounds when the original two surfaces are both irregular. To obtain an upper bound on the capacitance we consider that the original surfaces correspond to $S_1$ and $S_4$ and we consider specific $S_1$ and $S_3$ for which $C_{13}$ is known. To obtain our lower bound we consider that the original surfaces correspond to $S_2$ and $S_3$ and we consider specific surfaces $S_1$ and $S_4$ for which $C_{14}$ is known. For a large class of irregular surfaces the specific surfaces used to calculate the bounds can be spheres which are not necessarily concentric. The capacitance between non-concentric spheres will be treated in the next section. It should again be mentioned that the choice of spheres is only one possibility for using (12) to obtain upper and lower bounds.

## III. Capacitance of Nonconcentric Spheres

In this section we will derive an approximate expression for the capacitance between the two spheres depicted in figure 4. The radius of the outer sphere is b, the radius of the inner sphere is a, and the separation between the centers of the two spheres is c. An infinite series is given for this capacitance in the book by Smythe [5]. It is

$$C = 4\pi\varepsilon ab \sinh\alpha \sum_{n=1}^{\infty} [b \sinh(n\alpha) - a \sinh((n-1)\alpha)]^{-1} \tag{13}$$

where

$$\cosh\alpha = \frac{a^2+b^2-c^2}{2ab}, \qquad \alpha > 0 \tag{14}$$

We now introduce the normalized quantities

$$x = a/b \tag{15a}$$

$$y = c/b \tag{15b}$$

so that

$$x + y < 1 \tag{16}$$

and the capacitance of concentric spheres

$$C_o = \frac{4\pi\varepsilon a}{1-x} \tag{17}$$

so that (13) can be written as

$$C = C_o F \tag{18}$$

where

$$F = (1 - x)\sinh\alpha \cdot \sum_{n=1}^{\infty} (h_n)^{-1} \tag{19}$$

and

$$h_n = \sinh n\alpha - x \sinh(n - 1)\alpha \tag{20}$$

with

$$\cosh\alpha = \frac{1+x^2-y^2}{2x} \equiv \Gamma, \qquad \alpha > 0 \tag{21}$$

The normalized capacitance F was determined from the form given in (19) with the infinite sum terminated in the following manner. The $n^{th}$ term was compared to the sum of the preceeding n - 1 terms and when it was less than $10^{-8}$ of that sum, the series was terminated. The F obtained in this manner is plotted versus y for various x's.

We will now obtain a closed form analytic approximation to F. We write F as

$$F = (1 - x)S \tag{22}$$

where

$$S = \sum_{n=1}^{\infty} b_n \tag{23}$$

with

$$b_n = \frac{\sinh\alpha}{\sinh n\alpha - x \sinh(n-1)\alpha} \tag{24}$$

$$b_n = \frac{e^{\alpha}-e^{-\alpha}}{e^{n\alpha}-e^{-n\alpha}-x[e^{(n-1)\alpha}-e^{-(n-1)\alpha}]} \tag{25}$$

We now introduce a function $\delta(x,y)$ through the definition

$$\delta(x,y) = e^{-\alpha} - x \tag{26}$$

and use the fact that

$$e^{-\alpha} = \cosh\alpha - \sinh\alpha \tag{27}$$

or equivalently

$$e^{-\alpha} = \cosh\alpha - ((\cosh\alpha)^2 - 1)^{\frac{1}{2}}$$

$$\equiv \Gamma - (\Gamma^2 - 1)^{\frac{1}{2}} \tag{28}$$

with $\Gamma$ given in (21). Combining (21), (26), and (28) we find

$$\delta(x,0) = 0 \tag{29}$$

and

$$\frac{\partial\delta(x,y)}{\partial y} = \frac{y}{x}\,\frac{e^{-\alpha}}{\sinh\alpha} \geq 0 \tag{30}$$

From (29) and (30) we conclude, considering x as a parameter, that

$$\delta(x,y) \geq 0 \tag{31}$$

for arbitrary y. Solving for x in (26) and substituting it into (25) we obtain

$$b_n = \frac{e^{\alpha}(1-e^{-2\alpha})}{e^{n\alpha}(1-e^{-2\alpha})+2\delta\,\sinh(n-1)\alpha} \tag{32}$$

In view of (31) we have

$$b_n \leq c_n \tag{33}$$

where

$$c_n = (e^{-\alpha})^{n-1} \tag{34}$$

and the equality in (33) applies when $y = 0$. Returning to (22) and (23) we have

$$F \leq F_B \qquad (35)$$

where

$$F_B = (1 - x)S_B \qquad (36)$$

and

$$S_B = \sum_{n=1}^{\infty} c_n \qquad (37)$$

From (34) we see that $S_B$ is a geometric series which is readily summed to

$$S_B = (1 - e^{-\alpha})^{-1} \qquad (38)$$

Using (28) and (21) to obtain an explicit representation of $e^{-\alpha}$, we obtain after some simplifying algebra

$$S_B = \frac{1}{2}\left[1 + \left(\frac{(1+x)^2-y^2}{(1-x)^2-y^2}\right)^{\frac{1}{2}}\right] \qquad (39)$$

Perhaps the most convenient representation of $F_B$ is found by combining (36) and (39) to obtain

$$F_B = (\tfrac{1}{2})(1 - x)\left[1 + \left(\frac{(1+x)^2-y^2}{(1-x)^2-y^2}\right)^{\frac{1}{2}}\right] \qquad (40)$$

A form of $F_B$ that more readily exhibits the appropriate limit as y approaches zero is readily obtained from (40). It is

$$F_B = \frac{1}{2}[B + 1] + \frac{x}{2}[B - 1] \qquad (41)$$

where

$$B = \left(\frac{1-(y/1+x)^2}{1-(y/1-x)^2}\right)^{\frac{1}{2}} \qquad (42)$$

When y approaches 0, B approaches 1, and $F_B$ approaches 1 as it should.

It is found that $F_B$ is not only an upper bound on F, it is also a very good approximation to F over an appreciable range of x and y. This can be seen in the plots that we present of F and $F_B$.

## IV. Discussion of Results

The explicit capacitance bounds obtained in this note are presented in (1), (2), and (12), while a procedure for utilizing these bounds can be found in Section II. They are applied to the system of surfaces depicted in figure 1 as well as to bounding the capacitance to infinity of a single closed surface.

The numerical results for the normalized capacitance of the nonconcentric spheres are presented in figures 5 through 9. The quantity F represents (19), numerically summed, and the quantity $F_B$ is a closed form approximation to F given in (40). The capacitance for the nonconcentric spheres is obtained by using (17) to calculate the capacitance as though the spheres were concentric and then, according to (18), multiplying that quantity by F to obtain the actual capacitance. Thus, F is a measure of the increase in capacitance due to displacing the central sphere.

It should be noted that the scale of the ordinate in figures 5 through 9 is quite extended so that even though the curves appear to rise rapidly, the actual deviation of the capacitance from the concentric case increases slowly as the displacement of the central sphere is increased. This effect of the displacement is increased as the ratio of the two spheres becomes larger. Finally, it should be noted that another result is somewhat obscured by this extended scale. This is the degree to which $F_B$ approximates F. The maximum error that would result from using $F_B$ rather than F for the range of parameters depicted in these figures is as follows: 1.2%, 1.8%, 2.5%, 3.3%, and 4.2% for figures 5 through 9, respectively.

Appendix

In the region between the two surfaces depicted in figure 1 we satisfy

$$\underline{E} = -\nabla\phi \tag{A.1}$$

and

$$\nabla^2\phi = 0 \tag{A.2}$$

Integrating the identity

$$\nabla\cdot[\phi\nabla\phi] = \phi\nabla^2\phi + |\nabla\phi|^2 \tag{A.3}$$

over this region and using (A.2) as well as the divergence theorem, we obtain

$$\int_{S_1} dS\phi_1(-\hat{n}_1\cdot\nabla\phi) + \int_{S_2} dS\phi_2(-\hat{n}_2\cdot\nabla\phi) = \int_{R_{12}} d\underline{r}|\nabla\phi|^2 \tag{A.4}$$

We now consider the inner surface grounded and the outer surface to be at a potential $\phi_2 = V$. We also introduce the surface charge density $\sigma$ as

$$\sigma = \hat{n}_2\cdot\varepsilon\underline{E} = -\varepsilon\hat{n}_2\cdot\nabla\phi \tag{A.5}$$

Equation (A.4) now becomes

$$(1/\varepsilon)V\int_{S_2} dS\sigma = \int_{R_{12}} d\underline{r}|\nabla\phi|^2 \tag{A.6}$$

Using the fact that the total charge on $S_2$, q, is given by

$$q = \int_{S_2} dS\sigma \tag{A.7}$$

as well as the definition of capacitance

$$C_{12} = \frac{q}{V} \tag{A.8}$$

we obtain

$$C_{12} = (\varepsilon/V^2) \int_{R_{12}} d\underline{r} |\nabla\phi|^2 \tag{A.9}$$

Let us now define a new solution to Laplace's equations, $\phi'$, given by

$$\phi = V\phi' \tag{A.10}$$

It follows that $\phi' = 0$ on $S_1$ and $\phi' = 1$ on $S_2$. Substituting (A.10) into (A.9) and dropping the prime for convenience we have

$$C_{12} = \varepsilon \int_{R_{12}} d\underline{r} |\nabla\phi|^2 \tag{A.11}$$

where $\phi$ satisfies

$$\nabla^2\phi(\underline{r}) = 0 \qquad \underline{r} \in R_{12} \tag{A.12}$$

$$\phi(\underline{r}) = \begin{cases} 1 & \underline{r} \in S_1 \\ 0 & \underline{r} \in S_2 \end{cases} \tag{A.13}$$

One can see from this derivation that the choice of which surface to consider grounded does not effect $C_{12}$.

The following portion of this appendix is essentially an elaboration of some material contained in a book by Dettman [7]. Consider the following quadratic functional

$$Q(f) = \int_{R_{12}} d\underline{r} |\nabla f|^2 \tag{A.14}$$

where $R_{12}$ is as before. The class of functions $\{f\}$ over which we would like to minimize $Q(f)$ are those functions continuous in $R_{12}$ as well as on $S_1$ and $S_2$, with piecewise continuous first derivatives in $R_{12}$, and satisfying the boundary conditions $f = 0$ on $S_1$ and $f = 1$ on $S_2$. First we prove that $Q(f)$ is positive-definite. Assume that it is not, then $Q(f) = 0$ implies $\nabla f = 0$ in $R_{12}$. This in turn implies that f is a constant in $R_{12}$, and on $S_1$ and $S_2$. This is not possible since f is required to assume different values on $S_1$ and $S_2$ and at the same time be continuous in $R_{12}$ and on $S_1$ and $S_2$. Thus, we conclude that Q(f) is positive-definite. Therefore,

$$\min Q(f) = \lambda > 0 \tag{A.15}$$

Next we want to prove that the function $f \equiv \phi$ which minimizes Q(f) is the one that satisfies Laplace's equation in $R_{12}$ as well as the conditions that the $\phi$ belongs to the class of admissible functions {f}. Assume a solution $\phi$ exists, then

$$Q(\phi) = \lambda \tag{A.16}$$

and

$$Q(\phi + \xi\eta) \geq \lambda \tag{A.17}$$

where $\xi$ is an arbitrary constant and $\eta$ is an arbitrary function that satisfies the same continuity requirements as do the members of {f}, but $\eta$ satisfies the boundary conditions that it vanish on both $S_1$ and $S_2$. We now expand

$$Q(\phi + \xi\eta) = Q(\phi) + 2\xi Q(\phi,\eta) + \xi^2 Q(\eta) \tag{A.18}$$

where

$$Q(\phi,\eta) = \int_{R_{12}} d\underline{r} \nabla\phi \cdot \nabla\eta \tag{A.19}$$

Substituting (A.18) into (A.17) and using (A.16) to cancel the $\lambda$, we obtain

$$\xi^2 Q(\eta) \geq -2\xi Q(\phi,\eta) \tag{A.20}$$

with $\xi$ being an arbitrary constant. We will now show that (A.20) implies that

$Q(\phi,\eta) = 0$. First assume $Q(\phi,\eta) < 0$, then

$$\xi^2 Q(\eta) \geq 2\xi |Q(\phi,\eta)| \tag{A.21}$$

and this cannot be satisfied for arbitrarily small $\xi$. Finally assume $Q(\phi,\eta) > 0$, then define $\xi = -\delta$ with $\delta > 0$ and we have

$$\delta^2 Q(\eta) \geq 2\delta Q(\phi,\eta) \tag{A.22}$$

which also cannot be satisfied for arbitrarily small $\delta$. Thus we are left with the only possibility

$$Q(\phi,\eta) = 0 \tag{A.23}$$

We now integrate the vector identity

$$\nabla\cdot(\eta\nabla\phi) = \eta\nabla^2\phi + \nabla\eta\cdot\nabla\phi \tag{A.24}$$

over $R_{12}$, and use the divergence theorem and the definition of $Q(\phi,\eta)$ given in (A.19) to obtain

$$Q(\phi,\eta) = -\int_{R_{12}} d\underline{r}\,\eta\nabla^2\phi - \int_{S_1} dS\,\eta\hat{n}\cdot\nabla\phi - \int_{S_2} dS\,\eta\hat{n}\cdot\nabla\phi \tag{A.25}$$

Using the fact that $\eta$ vanishes on $S_1$ and $S_2$ as well as our derived result (A.23), we obtain

$$\int_{R_{12}} d\underline{r}\,\eta\nabla^2\phi = 0 \tag{A.26}$$

Since (A.26) must be satisfied by an arbitrary function $\eta$, we conclude that the $\phi$ which minimizes $Q(f)$ and which is a member of $\{f\}$ must also satisfy

$$\nabla^2\phi(\underline{r}) = 0 \qquad \underline{r} \in R_{12} \tag{A.27}$$

It should be noted that the proof would be unchanged if we considered the class of functions which had the same continuity properties as those in {f} but which vanished on $S_2$ and took the value one on $S_1$.

To summarize we have proved

$$\int_{R_{12}} d\underline{r}\,|\nabla\phi|^2 \leq \int_{R_{12}} d\underline{r}\,|\nabla f|^2 \qquad \text{(A.28)}$$

where both $\phi$ and f belong to {f} and $\phi$ in addition satisfies Laplace's equation in $R_{12}$. Multiplying both sides of (A.28) by $\varepsilon$ and recalling (A.11) through (A.13) we obtain

$$C_{12} \leq \varepsilon \int_{R_{12}} d\underline{r}\,|\nabla f|^2 \qquad f \in \{f\} \qquad \text{(A.29)}$$

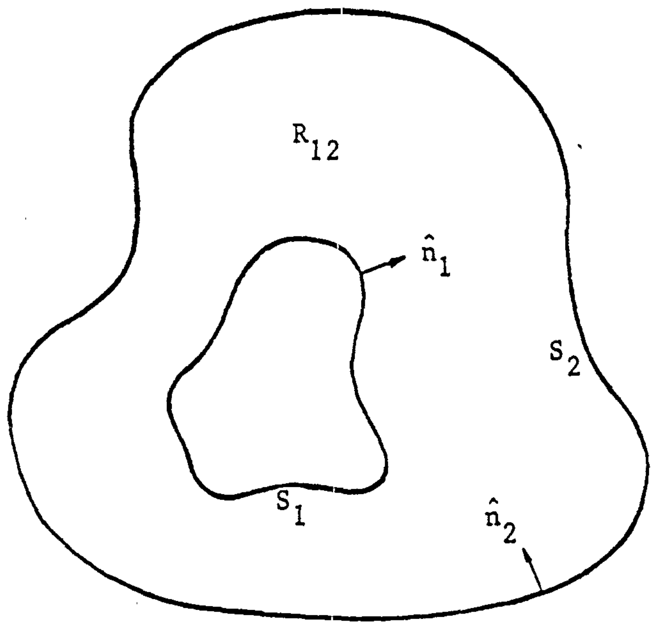


Figure 1. Arbitrary surface enclosing an arbitrary surface.

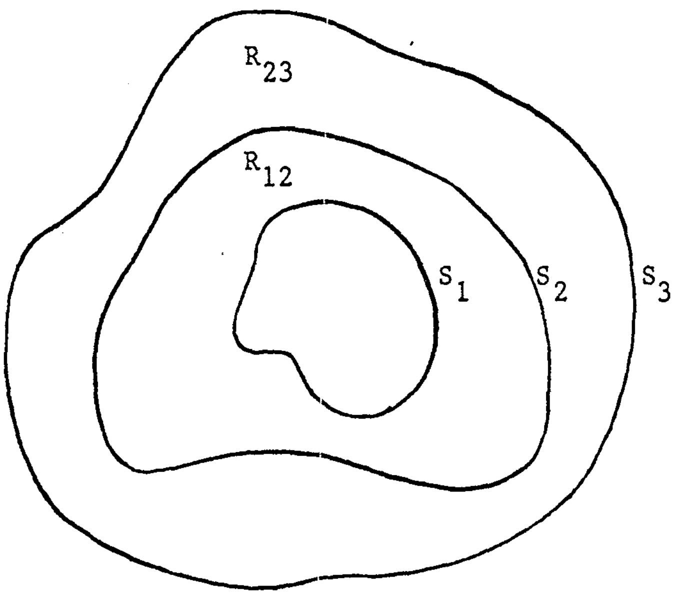


Figure 2. Three arbitrary surfaces.

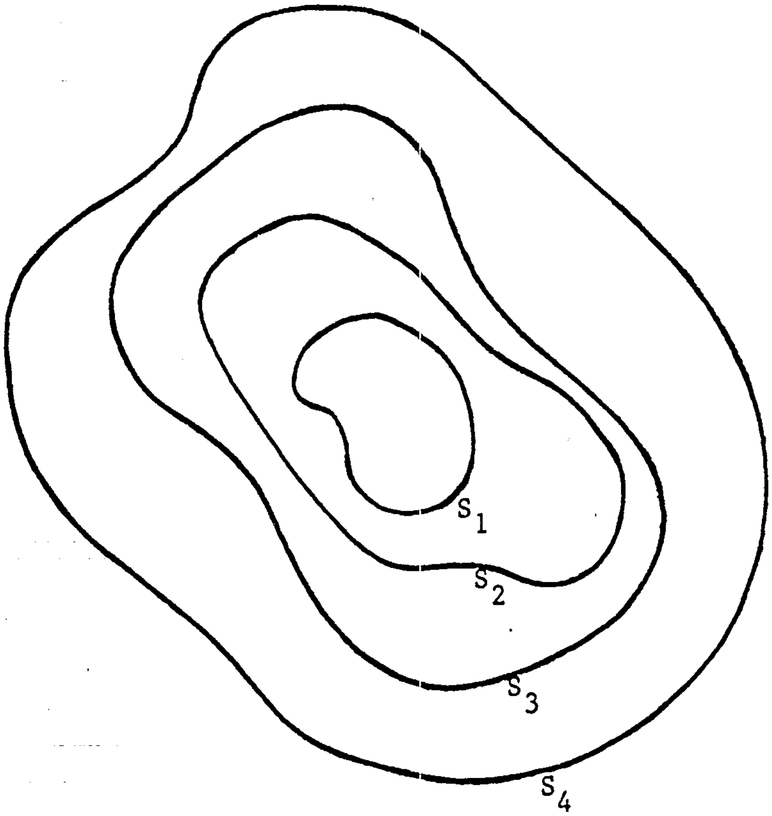


Figure 3. Four arbitrary surfaces

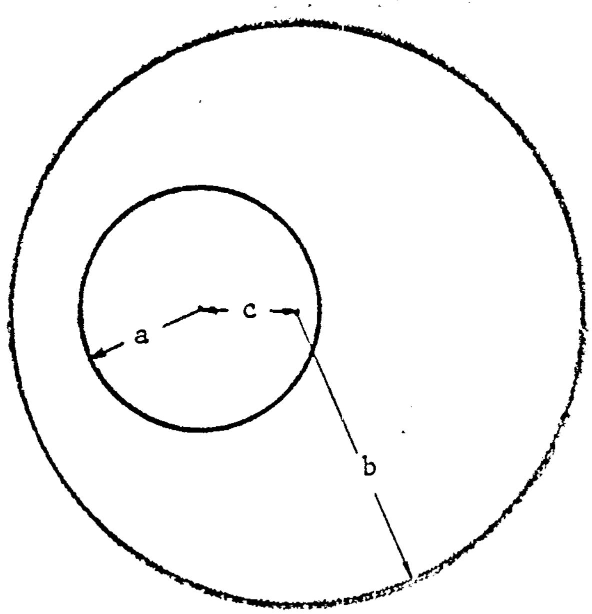


Figure 4. Nonconcentric spheres.

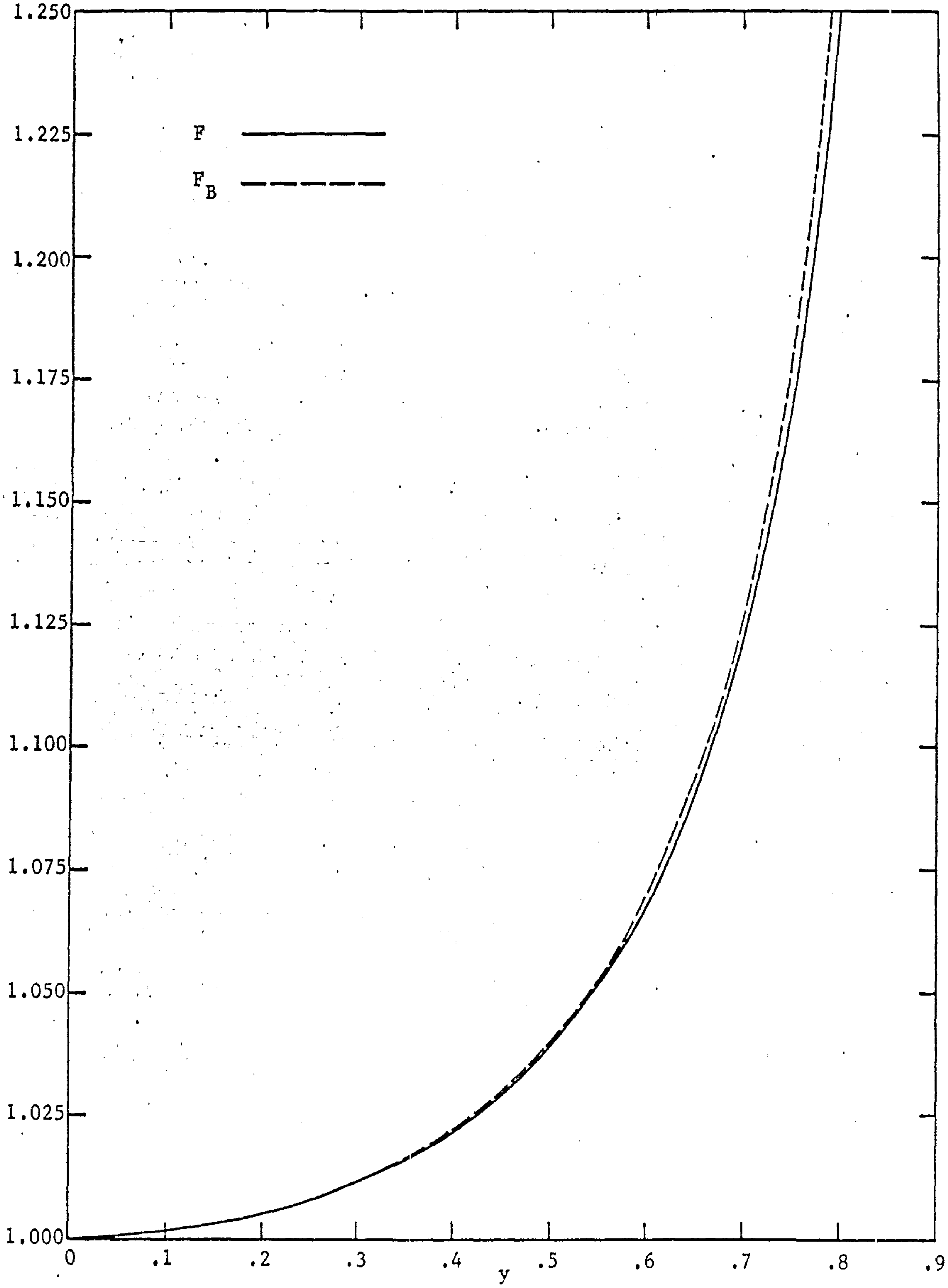


Figure 5. Normalized capacitance, F, and approximate normalized capacitance, $F_B$, versus normalized displacement of the central sphere, y, for the ratio of the radii of the spheres, x = .1.

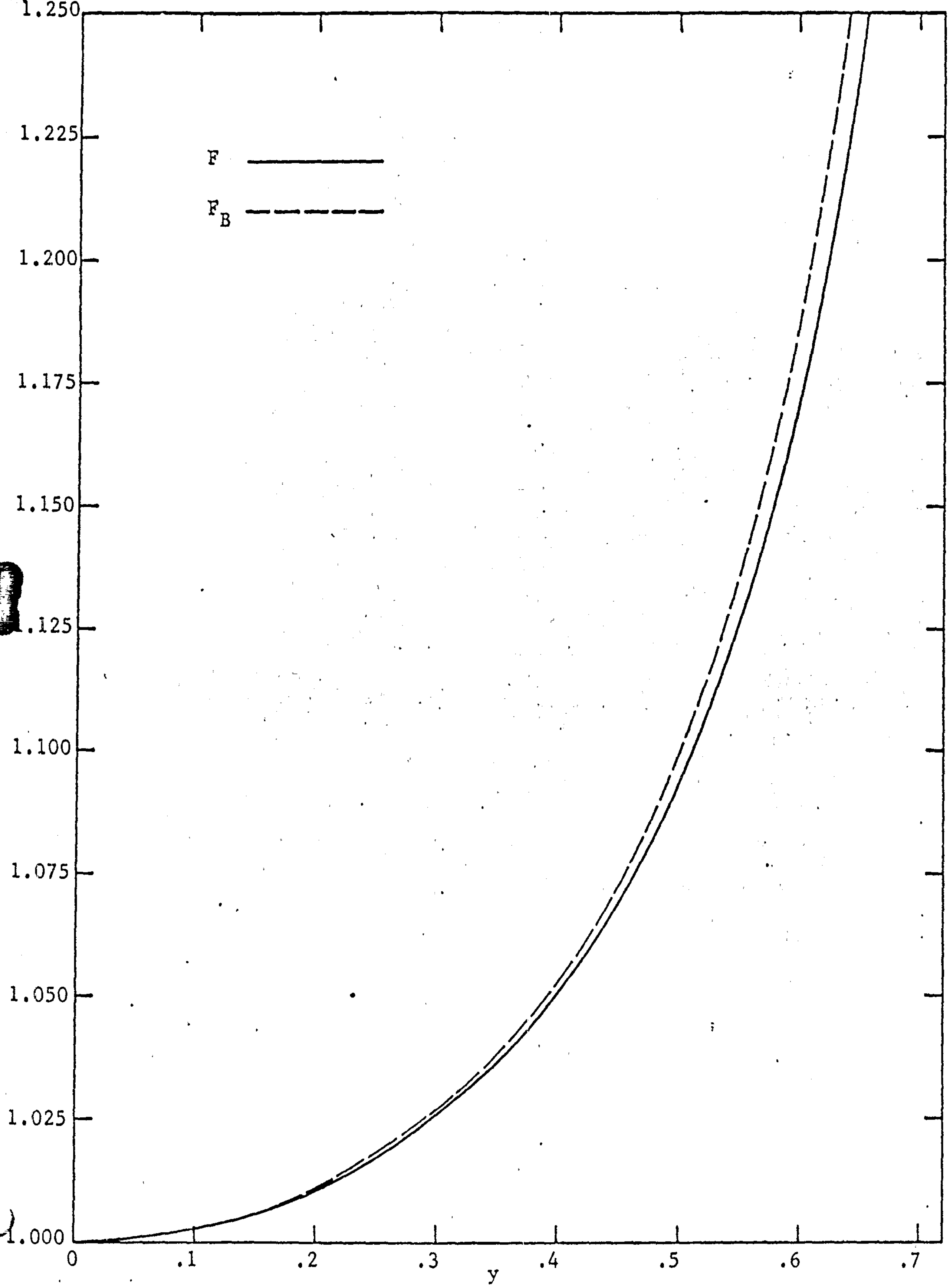


Figure 6. Normalized capacitance, F, and approximate normalized capacitance, $F_B$, versus normalized displacement of the central sphere, y, for the ratio of the radii of the spheres, x = .2.

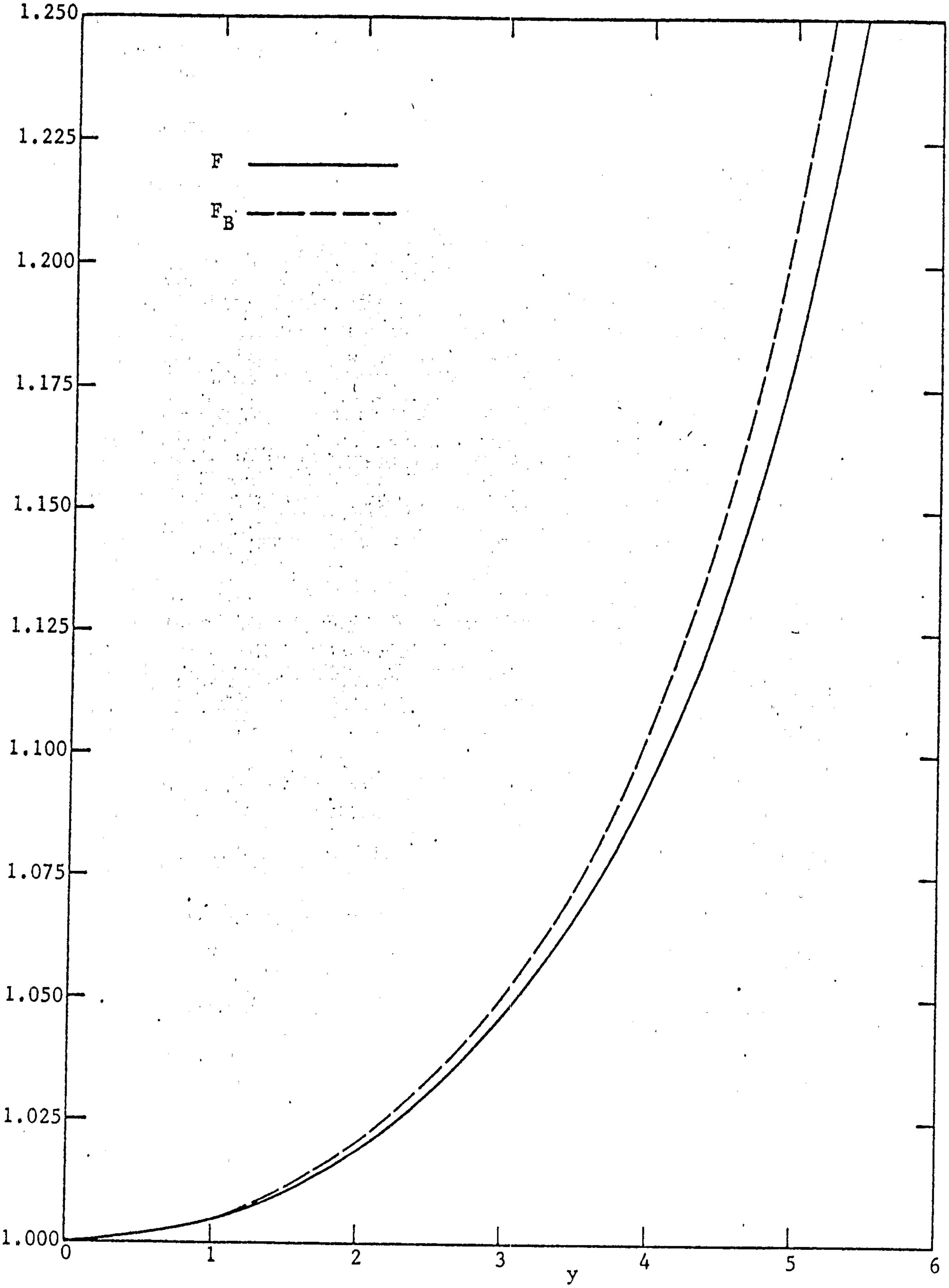


Figure 7. Normalized capacitance, F, and approximate normalized capacitance, $F_B$, versus normalized displacement of the central sphere, y, for the ratio of the radii of the spheres, x = .3.

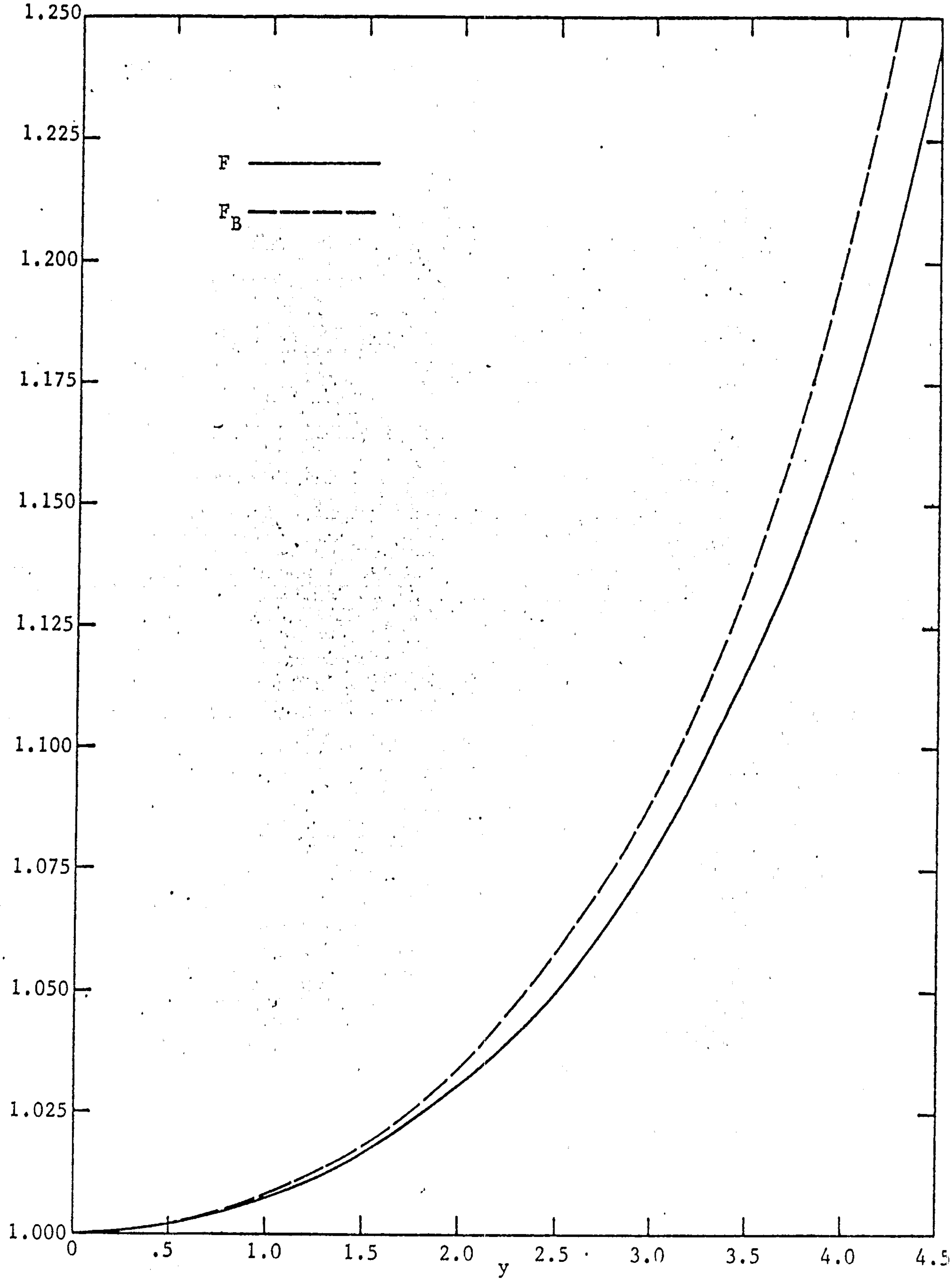


Figure 8. Normalized capacitance, $F$, and approximate normalized capacitance, $F_B$, versus normalized displacement of the central sphere, $y$, for the ratio of the radii of the spheres, $x = .4$.

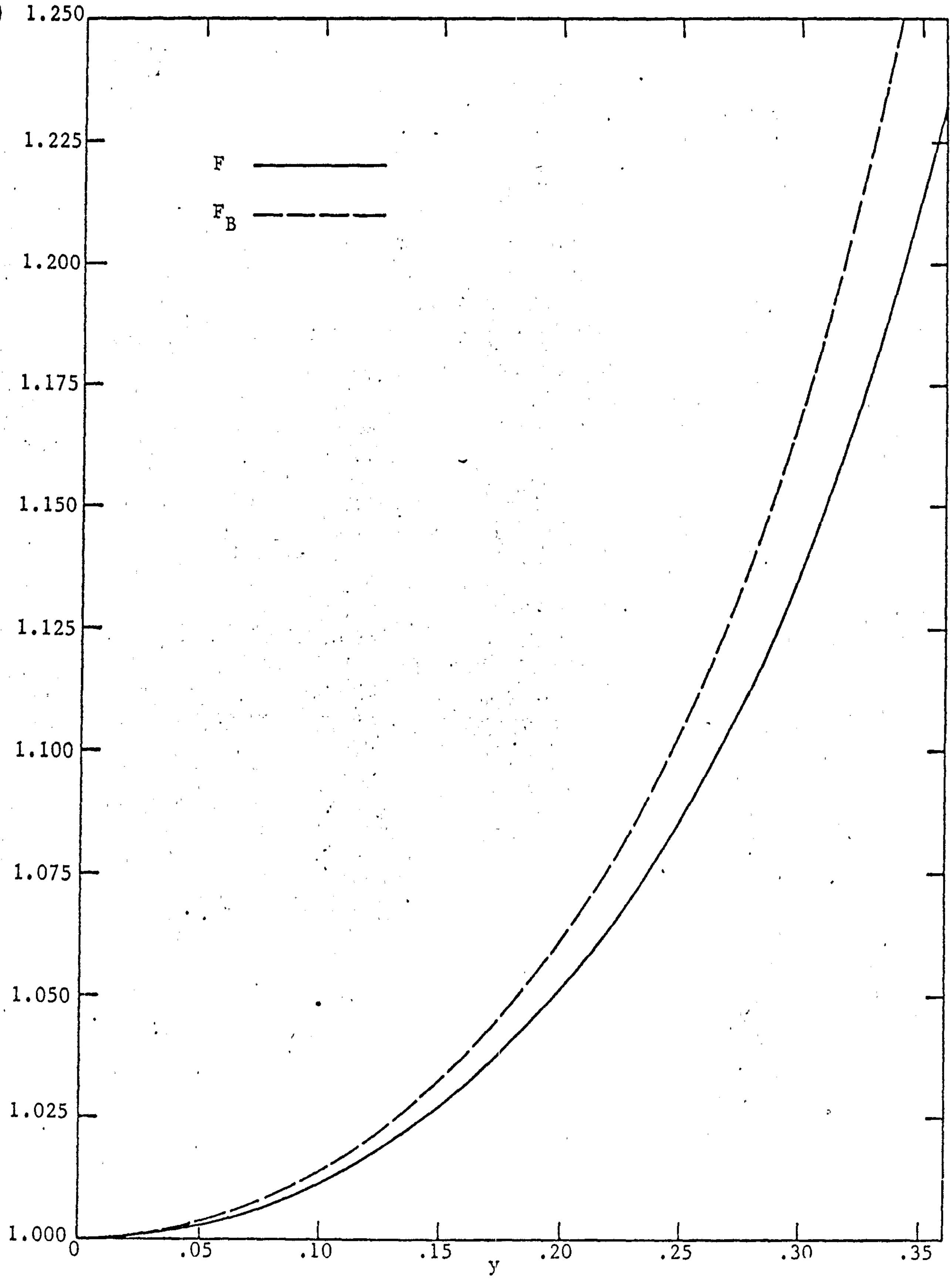


Figure 9. Normalized capacitance, F, and approximate normalized capacitance, $F_B$, versus normalized displacement of the central sphere, y, for the ratio of the radii of the spheres, x = .5.

## Acknowledgement

We thank Dr. R. Latham for his interest and for his help in programming, Dr. C. E. Baum for encouraging this study and for his support, and we also thank Mrs. G. Peralta for typing the manuscript.

References

1. C. E. Baum, "A Technique for Simulating the System Generated Electromagnetic Pulse Resulting from an Exoatmospheric Nuclear Weapon Radiation Environment," Sensor and Simulation Notes, Note 156, November 1972.

2. R. W. Latham, "The Effective Radii Approximation for the Capacitance of a Body Within an Enclosure," Sensor and Simulation Notes, Note 166, January 1973.

3. G. Pólya and G. Szegö, Isoparametric Inequalities in Mathematical Physics, Ann. of Math. Studies, No. 27, Princeton University Press, 1951.

4. W. E. Parr, "Upper and Lower Bounds for the Capacitance of the Regular Solids," J. Soc. Indust. Appl. Math., Vol. 9, No. 3, p. 334, September 1961.

5. W. R. Smythe, Static and Dynamic Electricity, McGraw-Hill, New York, 1950.

6. T. H. Shumpert, "Capacitance Calculations for Satellites," Sensor and Simulation Notes, Note 157, September 1972.

7. J. W. Dettman, Mathematical Methods in Physics and Engineering, McGraw-Hill, New York, 1962.